J Mater Sci (2011) 46:4413–4419
DOI 10.1007/s10853-010-5076-1

IIB 2010

Blunt corners of WC grains induced by lowering carbon content in WC–12mass%Co cemented carbides

I. Sugiyama · M. Goto · T. Taniuchi · F. Shirase · T. Tanase · K. Okada · Y. Ikuhara · T. Yamamoto

Received: 30 August 2010 / Accepted: 10 November 2010 / Published online: 14 January 2011

Abstract Habit planes at WC/Co interfaces were investigated from a viewpoint of carbon content in WC–12mass%Co cemented carbides by transmission electron microscopy (TEM). WC/Co interfaces typically consist of (0001) and $\{10\bar{1}0\}$ habit planes with blunt corners, which are very close to $\{10\bar{1}1\}$ habit plane. The sizes of the blunt corners increase as the carbon content decrease. The expansions of blunt corners are due to the change in interface energy caused by the variation of the carbon content. The change in interface energy is discussed in terms of the incoherency between the (0001) planes of the WC grains and the Co-phase.

I. Sugiyama (✉) · T. Yamamoto
Department of Advanced Materials Science, University of Tokyo, 5-1-5, Kashiwanoha, Kashiwa-shi, Chiba 277-8561, Japan
e-mail: sugiyama@sigma.t.u-tokyo.ac.jp

T. Yamamoto
e-mail: yamatala@k.u-tokyo.ac.jp

M. Goto · Y. Ikuhara
Engineering Research Institute, The University of Tokyo, 2-11-16, Yayoi, Bunkyo-ku, Tokyo 113-8656, Japan

T. Taniuchi · F. Shirase · K. Okada
Tsukuba Plant, Mitsubishi Materials Corp, 1511 Furumagi, Joso-shi, Ibaraki 300-2795, Japan

T. Tanase
Japan New Metal Co, 1-6-64, Sen-nari-cho, Toyonaka-shi, Osaka, Japan

Introduction

WC–Co-based cemented carbides are composites of hard WC grains bound by a Co-based binder γ-phase. Cemented carbides exhibit high hardness and high strength and are widely used in various tools for cutting, wire-drawing, mining, and so on. To obtain desirable mechanical properties in the alloys, it is necessary to control the WC grain size [1]. For this purpose, other carbides are often doped as grain growth inhibitors [2]. The typical carbides are VC and Cr_2C_3, which largely decrease the WC grain sizes [3]. According to previous reports, the structures at the WC/Co interfaces change as a result of doping with such inhibitors [4–7]. Yamamoto et al. [4] reported that particular structures appear at the interface of WC grains and Co-phase in VC-doped cemented carbides. In general, WC grains are hexagonal prismatic shapes whose habit planes are (0001) and $\{10\bar{1}0\}$. By doping VC, a very fine stairs-like structure is formed. The formation of this structure is closely related to the segregation of doped VC, which strongly retards step migration on the surface of WC grains during sintering.

On the other hand, the WC grain size can also be changed without the use of such inhibitors. The cemented carbides are generally fabricated by liquid-phase sintering, which is carried out above the eutectic temperature in the ternary system of W, C, and Co. During liquid-phase sintering, the carbon content in the alloys must be controlled in a two-phase region of WC and Co-phase to escape the appearance of free carbon or η-phase because these two phases are fatal to the mechanical properties of the cemented carbides [8]. In the ternary system of W, C, and Co, there exists an allowed range of the carbon content that keeps the phases in the two-phase region. In this carbon range, the WC grain size changes with variation of the

carbon content. According to a previous report, the size of WC grains becomes smaller when the carbon content is decreased, even in the cemented carbide without any inhibitors. For example, Suzuki et al. [9] reported that the WC grain size changes from 2.2 μm in a high carbon alloy to 1.6 μm in a low carbon alloy sintered at 1400 °C. Although the details have not been clarified yet, the grain growth behavior should be closely related to the interface structural change induced by the variation of the carbon content at liquid–solid interfaces. There are a few reports about WC–Co interfaces in the alloys of different carbon contents [10–12]; however, they are not enough to clarify the grain growth behavior.

In this study, the WC–Co interfaces were observed by transmission electron microscopy (TEM) for WC–12mass%Co cemented carbides with low and high carbon content. We provide some discussion from the view point of interface energy.

Experimental procedure

Two kinds of alloys were prepared by the ordinary liquid-phase sintering method. The nominal compositions of the alloys were WC–12mass%Co with their carbon contents controlled close to the lower and higher limits of carbon content in the two-phase region of WC and γ-phases. In what follows, these carbides will be denoted as LC and HC, respectively. The raw powders of WC (Japan New Metals Co. Ltd., nominal grain size of 0.8 μm) and Co (Umicore Co. Ltd., 1.4 μm) were weighed to be target composition, and then attritor-milled, dried, and pressed into a shape of $16 \times 16 \times 5$ mm^3 under a pressure of 150 MPa. After that, the green compacts were sintered at 1380 °C for 1 and 5 h in vacuum. After sintering, all specimens were rapidly cooled by introducing He gas into the furnace. Scanning electron microscope (SEM, H-S800, Hitachi Co. Ltd., Japan) observation and saturated magnetization measurements were then performed to confirm the carbon content.

The microstructure was investigated by a transmission electron microscope (EM-002BF, Topcon Co. Ltd.). A conventional ion-milling technique with an Ar ion beam was used for TEM sample preparation, in addition to mechanical grinding and polishing process.

Results

Alloys sintered for 1 h

Figure 1 shows TEM bright field images of alloys sintered for 1 h. As previously reported [9], WC grains are smaller in the LC alloy compared to the HC alloy. This confirms that a variation of carbon content changes the WC grain size. Most of the WC grains have a hexagonal prismatic shape whose basal plane is (0001) and prismatic plane is $\{10\bar{1}0\}$. When an electron beam is set along the $[11\bar{2}0]$ direction of a WC grain, we see the WC grain as a rectangle whose sides are (0001) and $\{10\bar{1}0\}$. As WC grains often grow anisotropically [12, 13], the interface at (0001) is wider than the interface at $\{10\bar{1}0\}$ on the rectangle. This anisotropic growth becomes remarkable in the HC alloy, as in previous studies [10, 12, 13].

Figure 2 shows TEM bright field images at the corner of WC grains in the alloys sintered for 1 h, which were taken from the $[11\bar{2}0]$ direction of the respective WC grains. As seen in the images, the WC grains exhibit clear habit planes of (0001) and $\{10\bar{1}0\}$, which are typical habits in WC–Co-based cemented carbides. However, there can be seen a distinct feature at the corner of the two habits. The corner of the two habits, indicated by an arrow, is very sharp in the HC alloy, whereas it is not sharp in the LC alloy. A similar shape was also reported by Wang et al. [10]. In the LC alloy, the two habits can be considered not to grow fully, even during liquid-phase sintering.

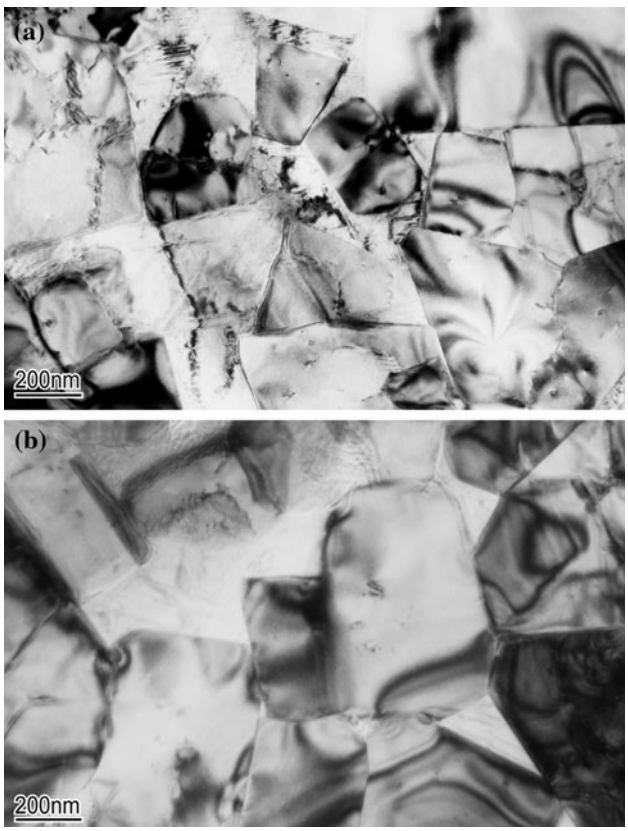

Fig. 1 TEM bright field images in **a** LC and **b** HC alloys sintered for 1 h

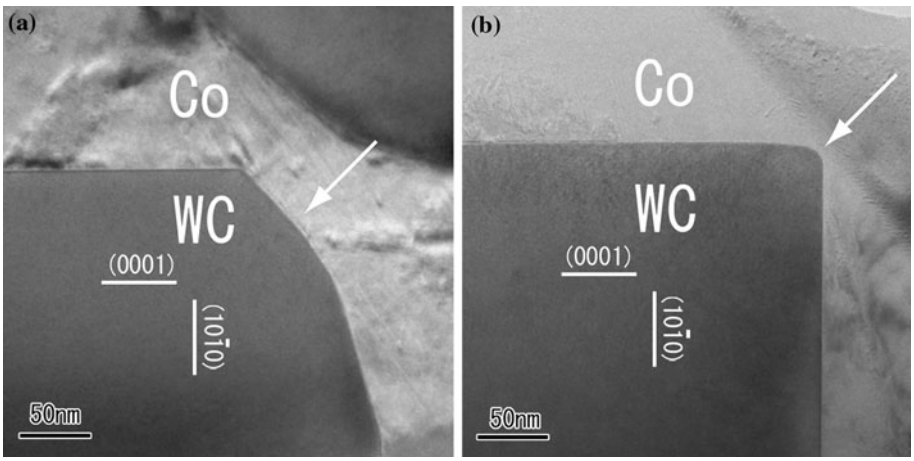

Fig. 2 Magnified TEM bright field images at the corner of WC grain in **a** LC and **b** HC alloys sintered for 1 h. *Arrows* show corners of WC grains

Alloys sintered for 5 h

Figure 3 shows TEM bright field images of the alloys sintered for 5 h. In each alloy, the size of the WC grains becomes larger compared with that in the alloys sintered for 1 h. The LC alloy exhibits a smaller grain size than the HC alloy even after the sintering time was prolonged.

Figure 4 shows TEM bright field images at the corners of WC grains in the alloys sintered for 5 h. After sintering for long time, the LC alloy still shows a blunt corner between the two habit planes, indicating that the shape particular to LC alloys can be considered to be an equilibrium shape. Hereafter, we shall refer to the plane which appears at the corner as the oblique habit.

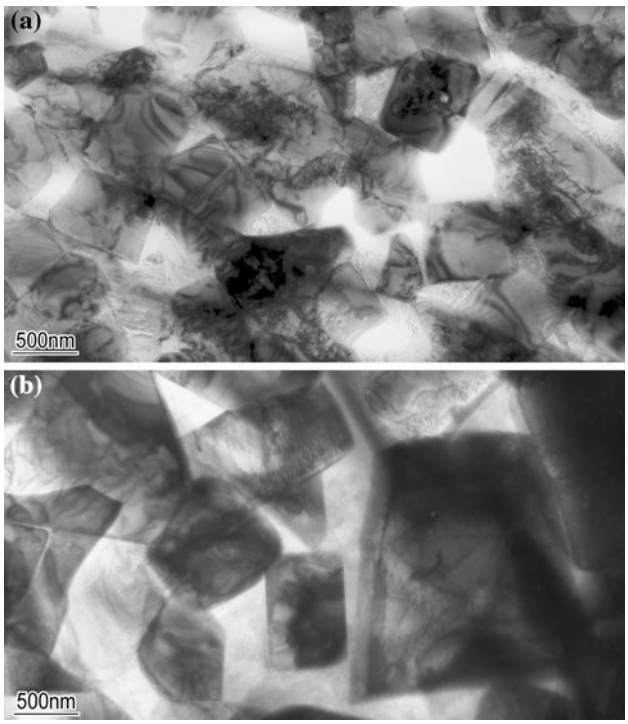

Fig. 3 TEM bright field images in **a** LC and **b** HC alloys sintered for 5 h

Discussion

Interface energy of the (0001) and {10$\bar{1}$0} habits in the high and low carbon limit

To discuss the appearance of the oblique habit, it is necessary to know the change of the interface energy at the (0001) and {10$\bar{1}$0} habits induced by the change of the carbon content. Christensen et al. [14, 15] calculated the carbon content dependency of the interface energy by DFT at (0001) and at {10$\bar{1}$0}. To construct supercells, they considered four types of translations and two types of terminations for the respective translations at (0001), and three types of translations and two types of terminations at {10$\bar{1}$0}. For {10$\bar{1}$0}, they further included two types of stacking sequences due to crystallographic anisotropy at {10$\bar{1}$0}and {10$\bar{1}$0}. The DFT calculations were carried out for the respective structures in two carbon activity. One is the carbon content limit at η-phase, which corresponds to the LC alloy in this study, and the other is the limit of free carbon, which corresponds to the HC alloy. To describe various misorientations between WC grain and Co-phase, they introduced a parameter of α as follows,

$$\gamma = \gamma_{\min} + \alpha(\gamma_{\max} - \gamma_{\min}), \quad (1)$$

where γ is the interface energy of the WC–Co interface, $\gamma_{\min}$ is the calculated lowest energy at the respective habits, and $\gamma_{\max}$ is the average of the interface energy calculated from all supercells at the respective habits. The parameter α shows the incoherency between the WC grain and the Co-phase. Figure 5 is a part of their result showing γ as a function of α at basal (0001) and prismatic {10$\bar{1}$0} planes.

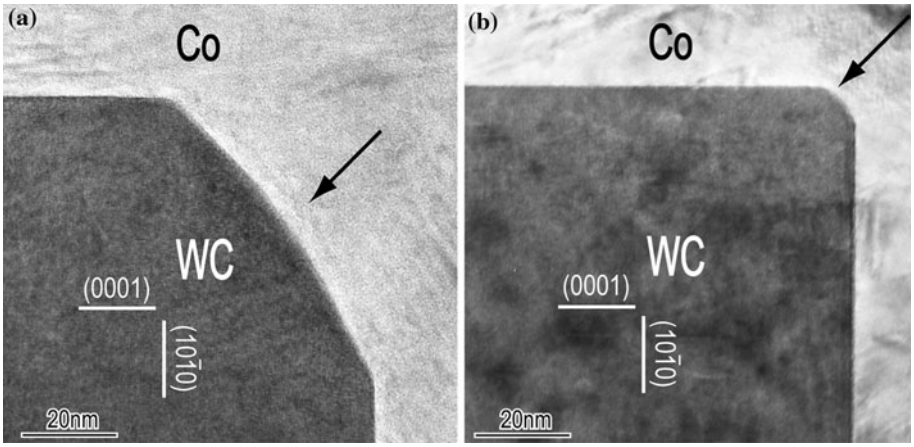

Fig. 4 Magnified TEM bright field images at the corner of WC grain in **a** LC and **b** HC alloys sintered for 5 h. *Arrows* show corners of WC grains

In the plot, the results of the lowest energy obtained at the carbon (HC) and tungsten (LC) limits are shown. The coherency limit is 0.818, 0.665, 0.671, and 0.888, and the incoherency limit is 1.50, 1.76, 2.31, and 2.53 J/m^2 for the basal plane W-rich limit, the basal plane C-rich limit, the prismatic W-rich limit, and the prismatic C-rich limit, respectively. As seen in the plot, the α dependency of the interface energy exhibits different features between (0001) and $\{10\bar{1}0\}$. In the case of $\{10\bar{1}0\}$, the interface energy is proportional to α irrespective of the carbon content. The energy change $\Delta\gamma$ with carbon content, i.e., $\gamma_m^{HC} - \gamma_m^{LC}$, where γ_m^{HC} and γ_m^{LC} denote the interface energy at $\{10\bar{1}0\}$ in HC and LC alloys, respectively, is constant against α. By reducing the carbon content, the interface energy is equally decreased at any α. In contrast, a cross point exists for the (0001) habit around $\alpha = 0.22$ because the most stable termination changes at the higher carbon limit. Due to the change of termination, the interface energy at (0001) does not largely change around $\alpha = 0.22$ even if the carbon content varies. The value of $\alpha = 0.22$ is very similar to that obtained experimentally. According to previous reports [11, 16], the orientation relationship of $[0001]_{WC}//[111]_{Co}$ is observed most frequently by TEM observation. This orientation has a misfit of 15%. This means rather poor coherency [13]. Lay et al. experimentally estimated the incoherency to be smaller than 20% at (0001) [13]. Thus, the preferable incoherency is about 0.2. The important point is that the experimentally estimated α value is around the cross point as seen in the γ plot of (0001) in Fig. 5. Namely, the interface energy at (0001) exhibits only a small change even if the carbon content changes.

$\Delta\gamma$ of oblique habits

As shown in Figs. 2 and 4, an oblique habit is formed at the corner of (0001) and $\{10\bar{1}0\}$ planes in the LC alloy. The oblique habit can be considered to exist stably at an equilibrium state because the habits can also be seen after long time sintering, as shown in Fig. 4. The appearance of the oblique habit means that the interface energy at WC–Co varies with the carbon content. To understand the details of the relationships among the interface energies at the respective habits, the energetic difference due to a change in the carbon content must be considered.

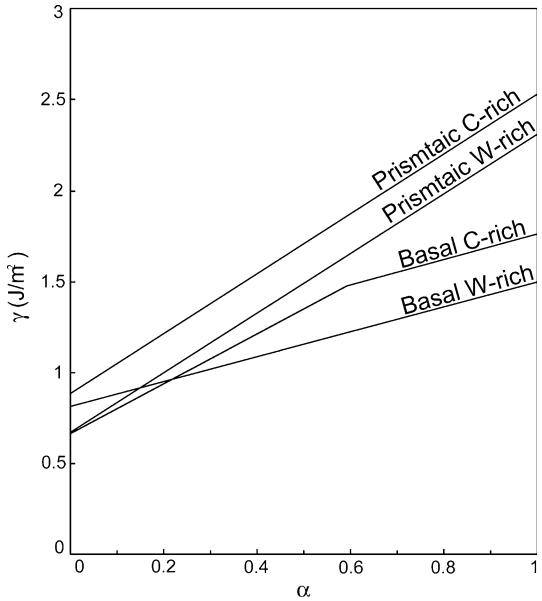

Fig. 5 WC/Co interface energy of basal (0001) habit and prismatic $\{10\bar{1}0\}$ habit plotted against incoherency α [15]. W-rich and C-rich represent LC and HC in this study, respectively

According to Christensen et al. [14, 15], the interface energy is expressed by the following equation,

$$\gamma = \frac{1}{A}[E - \mu_{WC}N_W + \mu_C(N_W - N_C) - \mu_{Co}N_{Co}], \quad (2)$$

where A, E, N, and μ are the total area of the interface in the system, the total energy of the system, the numbers of W, C, and Co atoms in the system, and the chemical potential of WC, C, and Co, respectively. Here, μ_C, μ_W, μ_{Co}, N_W, N_C, and N_{Co} are independent of the type of habit,

though some of them have a carbon content dependency. In contrast, A and E depend on the type of habit, but not on the carbon content. Thus, Eq. 2 can be divided into a no carbon dependency term and a term that depends on carbon content as follows,

$$\gamma = \frac{E}{A} + \frac{f_{(C)}}{A}, \tag{3}$$

where $f_{(C)}$ is a term that depends on carbon content as follows,

$$f_{(C)} = -\mu_{WC}N_W + \mu_C(N_W - N_C) - \mu_{Co}N_{Co} \tag{4}$$

Thus, the difference in the interface energy, $\Delta\gamma$, between the two carbon limits is

$$\Delta\gamma = \gamma^{HC} - \gamma^{LC} = \frac{f^{HC}_{(C)} - f^{LC}_{(C)}}{A}, \tag{5}$$

where $f^{HC}_{(C)}$ and $f^{LC}_{(C)}$ are $f_{(C)}$ in the HC and LC alloys, respectively. All the terms in $f_{(C)}$ have no relation to the type of habit. Therefore, $\Delta\gamma$ is dependent only on A irrespective of habits when the termination does not change. Under the conditions used in Ref. [14, 15], A can be expressed as a function of the area in the unit cell of the WC lattice. The ratio of A at the (0001) and $\{10\bar{1}0\}$ planes is 1.1. This value is equal to the value of $\Delta\gamma_c/\Delta\gamma_m$ calculated by the data of Christensen et al. in the condition that the termination does not change between the HC and LC alloys. Here, the subscripts c and m denote the (0001) and $\{10\bar{1}0\}$ planes, respectively. Thus, $\Delta\gamma$ of the oblique habit should be smaller than that of (0001) and $\{10\bar{1}0\}$ because A of the oblique habit is larger than those of the two habits.

Appearance of oblique habits

The interface energy at the corner of WC grains without and with oblique habits can be written, respectively, as follows,

$$S_c\gamma_c + S_m\gamma_m \tag{6}$$

$$S_o\gamma_o\left[1 + \frac{S_cS_mA_o}{(S_C + S_M)S_o}\right], \tag{7}$$

where S_c, S_m, S_o and γ_c, γ_m, γ_o are the areas at the corner of the WC grains and the interfacial energies of the (0001), $\{10\bar{1}0\}$ and oblique habits, respectively, as in Fig. 6. The respective subscripts of c, m, and o represent the (0001), $\{10\bar{1}0\}$ and oblique habits at the corner of WC grains. The bracketed expression in Eq. 7 is a correction term for the increase of the area at the oblique habit in the condition that the volume does not change by the appearance of oblique habits, as shown in Fig. 6. S_C and S_M are total areas of the (0001) and $\{10\bar{1}0\}$ planes, respectively.

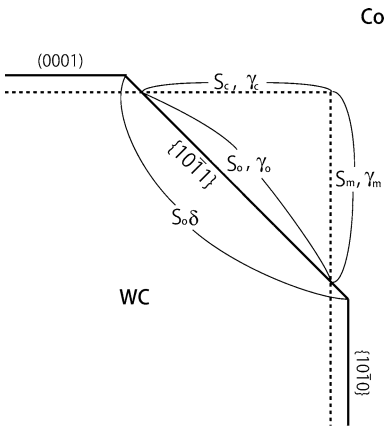

Fig. 6 A schematic at a corner of a WC grain. The *dotted line* represents the corner in HC alloys while the *continuous line* pertains to LC alloys. Here, the correction term in Eq. 7 is denoted as δ

As oblique habits exist stably in the LC and not in the HC limits, we obtain the following equations using Eqs. 6 and 7,

$$S_c\gamma_c^{HC} + S_m\gamma_m^{HC} < S_o\gamma_o^{HC}\left[1 + \frac{S_cS_mA_o}{(S_C + S_M)S_o}\right] \tag{8}$$

$$S_c\gamma_c^{LC} + S_m\gamma_m^{LC} > S_o\gamma_o^{LC}\left[1 + \frac{S_cS_mA_o}{(S_C + S_M)S_o}\right] \tag{9}$$

As shown in Figs. 2 and 4, the shape of the blunt corner does not change with annealing time and carbon content. So, in the analysis, the torque effects are not considered. Subtracting Eq. 9 from Eq. 8, the conditional equation for appearance of oblique habits by changing the carbon content can be written as follows,

$$S_c\Delta\gamma_c + S_m\Delta\gamma_m < S_o\Delta\gamma_o\left[1 + \frac{S_cS_mA_o}{(S_C + S_M)S_o}\right], \tag{10}$$

where using Eq. 3, $\Delta\gamma$ can be written as follows,

$$\Delta\gamma_c = \frac{\Delta f_{(C)}}{A_c},\ \Delta\gamma_m = \frac{\Delta f_{(C)}}{A_m} \text{ and } \Delta\gamma_o = \frac{\Delta f_{(C)}}{A_o} \tag{11}$$

Here, $\Delta f_{(C)}$ is calculated from $f^{HC}_{(C)} - f^{LC}_{(C)}$ and is independent from the type of habit. In Eq. 10, the ratio of S_c, S_m, and S_o is determined crystallographically because the angles between two of the (0001), $\{10\bar{1}0\}$, and oblique habits are crystallographically defined, and $\Delta\gamma_o$ is smaller than $\Delta\gamma_c$ and $\Delta\gamma_m$, as discussed in section "$\Delta\gamma$ of oblique habits." The correction term is close to 1 because the oblique habit is very small. In this condition, Eq. 10 cannot be valid because the left-hand side is much larger than the right-hand side. Thus, to make the Eq. 10 valid, we have to consider the α dependency of $\Delta\gamma_c$ at $\alpha < 0.6$ in Fig. 5 as discussed in section "Interface energy of the (0001) and $\{10\bar{1}0\}$ habits in the high and low carbon limit." Eq. 10 can be rewritten by correcting the term $S_c\Delta\gamma_c$ using the variable x ($x \geq 1$) as follows,

$$S_c\Delta\gamma_c \cdot x + S_m\Delta\gamma_m < S_o\Delta\gamma_o\left[1 + \frac{S_cS_mA_o}{(S_C + S_M)S_o}\right], \quad (12)$$

where x shows the difference of $S_c\Delta\gamma_c$ in a <0.59 as shown in Fig. 5. The relation between x and α is shown by $x = 2.69(\alpha - 0.22)$ $(0 < \alpha < 0.59)$ and $x = 1$ $(0.59 > \alpha)$. Dividing all terms by $\Delta f_{(C)}$, Eq. 12 can be rewritten using Eq. 11 as follows,

$$\frac{S_c}{A_c} \cdot x + \frac{S_m}{A_m} < \frac{S_o}{A_o}\left[1 + \frac{S_cS_mA_o}{(S_C + S_M)S_o}\right] \quad (13)$$

because $\Delta f_{(C)} > 0$.

Each value of A in Eq. 13 is obtained from the area of the respective planes in the unit cell. S_c, S_m, and S_o are obtained from a schematic as in Fig. 6, which are multiplied by the same constant. S_C and S_M are obtained by measuring the length of respective habits of the grain as shown, for example, in Fig. 7. Using these values, the following equations are obtained,

$$\frac{S_c}{A_c} = \frac{1}{1.453} \quad (14)$$

$$\frac{S_m}{A_m} = \frac{1}{2.906} \quad (15)$$

$$\frac{S_o}{A_o} = \frac{1}{2.906} \quad (16)$$

$$1 + \frac{S_cS_mA_o}{(S_C + S_M)S_o} = 1.199 \quad (17)$$

In this calculation, the blunt corner is taken to be consisting of only $\{10\bar{1}1\}$ habit plane as a simplification. This simplification is valid because other habits in the blunt corners are very close to $\{10\bar{1}1\}$, and this only affects little on the correction term. By substituting these values in Eq. 13, $x < 0.10$ can be obtained. As a result, α is smaller than 0.26, as in Fig. 5 for the case of the LC alloy. Similarly, $x > 0$ and α is larger than 0.22 from the HC alloy considering the very small oblique habits as seen in the experimental microstructure in Fig. 4b. It is notable that the α value calculated in this study roughly corresponds to the experimental value in previous reports [10, 12, 15]. Namely, the length of oblique habit can be calculated by the value of the incoherency between the (0001) planes of the WC grain and the Co-phase.

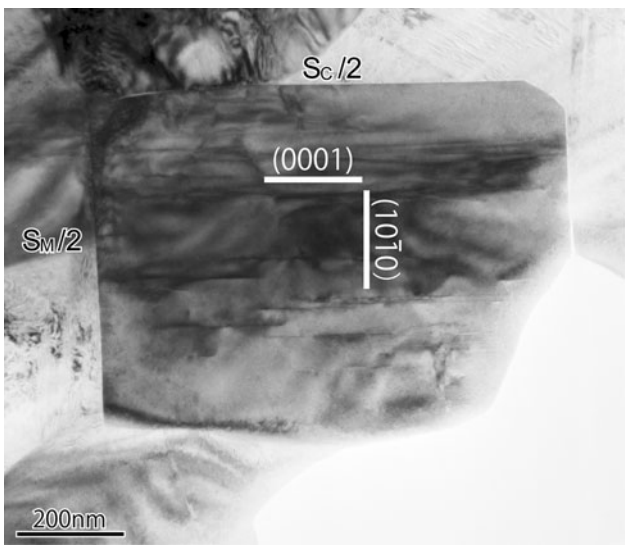

Fig. 7 A whole view of the WC grain shown in Fig. 4a

Conclusions

The shape of WC grains was investigated by TEM for WC–12mass%Co with high and low carbon content. In the case of high carbon alloys, WC grains exhibit a rectangular shape when viewed from the $[11\bar{2}0]$ direction with habit planes (0001) and $\{10\bar{1}0\}$. The corner of the two habits was sharp. In contrast, another habit plane appeared in low carbon alloys at the corner of the two habits. This additional habit exists stably even after the sintering time is prolonged. The appearance of this additional habit is due to a change of the energetic stabilization induced by lowering the carbon content. From a consideration of areas, the energetic stabilization supports the formation of a large oblique habit in the LC case, but only a very small habit in the HC case under the condition that the incoherency α is near 0.2. This value corresponds to the incoherent value which was estimated in previous studies [10, 12, 15] (see section 4.1). In conclusion, the grain morphology at the corner of WC grains is determined by the incoherency between the (0001) planes of the WC grains and the Co-phase.

Acknowledgements This study was supported by a grant-in-aid for scientific research for the priority area "Nano Materials science for atomic scale modification 474" 19053001 from the Ministry of Education, Culture, Sports, Science and Technology of Japan. Thanks to Dr. S. D. Findlay for helpful discussion.

References

1. Schubert WD, Bock A, Lux A (1995) Int J Refract Metals Hard Mater 13:281
2. Suzuki H, Fuke Y, Hayashi K (1972) J Jpn Soc Powder Powder Metall 19:26
3. Hayashi K, Fuke Y, Suzuki H (1972) J Jpn Soc Powder Powder Metall 19:37
4. Yamamoto T, Ikuhara Y, Sakuma T (2000) Sci Tech Adv Mater 1:97
5. Yamamoto T, Ikuhara Y, Watanabe T, Sakuma T, Taniuchi Y, Okada K, Tanase T (2001) J Mater Sci 36:3885. doi:10.1023/A:1017953701641
6. Lay S, Thibault J, Hamar-Thibault S (2003) Phil Mag 83:1175

7. Delanoë A, Bacia M, Pauty E, Lay S, Allibert CH (2004) J Crys Growth 270:219
8. Chaporova IN, Shchetilina EA (1954) Izv Akad Nauk SSSR Met Topl 5:91
9. Suzuki H, Sugiyama M, Umeda T (1964) J Jpn Soc Metall 28:55
10. Wang Y, Heusch M, Lay S, Allibert CH (2002) Phys Sol Stat 193:271
11. Bounhoure V, Lay S, Loubradou M, Missiaen JM (2008) J Mater Sci 43:892. doi:10.1007/s10853-007-2181-x
12. Delanoë A, Lay S (2009) Int J Refract Metals Hard Mater 27: 140
13. Lay S, Allibert CH, Christensen M, Wohnstrőm G (2008) Mater Sci Eng A 486:253
14. Christensen M, Wahnström G, Allibert C, Lay S (2005) Phys Rev Lett 96:066105
15. Christensen M, Wahnström G, Lay S, Allibert CH (2007) Acta Mater 55:1515
16. Mohan K, Strutt PR (1996) Mater Sci Eng A 209:237